The behavior of statically-indeterminate structural members and frames with cracks present

Paul C. Paris *, Thierry Palin-Luc

Arts et Metiers ParisTech, Universite Bordeaux 1, LAMEFIP, Esplanade des Arts et Métiers, F-33405 Talence Cedex, France

A B S T R A C T

Crack stability is discussed as affected by their presence in statically-indeterminate beams, frames, rings, etc. loaded into the plastic range. The stability of a crack in a section, which has become plastic, is analyzed with the remainder of the structure elastic and with subsequent additional plastic hinges occurring. The reduction of energy absorption characteristics for large deformations is also discussed. The methods of elastic–plastic tearing instability are incorporated to show that in many cases the fully plastic collapse mechanism must occur for complete failure.

Keywords:
J-integral
Plastic hinge
Tearing stability analysis
Crack stability
Elastic plastic crack growth
Energy dissipation

1. Introduction

Many safety critical structural members and frames incorporate materials with very high resistance to unstable fracture from cracks, existing or produced by mechanisms of fatigue, corrosion, etc. Under such circumstances, if the cracked section is later exposed to high loads, it can become fully plastic without crack instability. Nuclear reactor piping, civil buildings and bridges with welded steel beams and frames, offshore oil platforms, etc. are but a few examples. This paper shall assume that it is important to have the cracked section become fully plastic without unstable rapid fracture (the material is assumed tough enough to avoid sudden fracture). It is the objective here to show that for statically-indeterminate members the conditions for such behavior are often present and can be assured. The approach taken here will be the use of *J*-integral based tearing stability analysis to demonstrate the case for such behavior.

First, the basis of *J*-integral tearing stability method is presented hereafter. The second part of this paper is devoted to study the stability of a crack in a fixed ended beam with different typical cross-sections often used in mechanical engineering. Furthermore, one studies the effect, on the crack stability, of the elastic stiffness of the structure where the beam is fixed. All these cases lead to simple analytic equations to assess the effective length of the beam. A third part is focused on some special statically indeterminate structures. Then, the material properties needed to assure crack stability are discussed. The work dissipated by plastic collapse mechanism with crack present is calculated in the case of one of the special frames previously studied and for the fixed ended beam with different sections. Finally, the ratio between the limit bending moment at a cracked section and the uncracked plastic hinge moment of sections is considered.

* Corresponding author. Home address: 128 Sundown Rdg., Maryville, IL-62062, USA. Tel.: +1 314 630 9948; fax: +1 314 935 4014.
E-mail addresses: pcparis30@gmail.com (P.C. Paris), thierry.palin-luc@ensam.eu (T. Palin-Luc).

doi:10.1016/j.engfracmech.2009.05.001

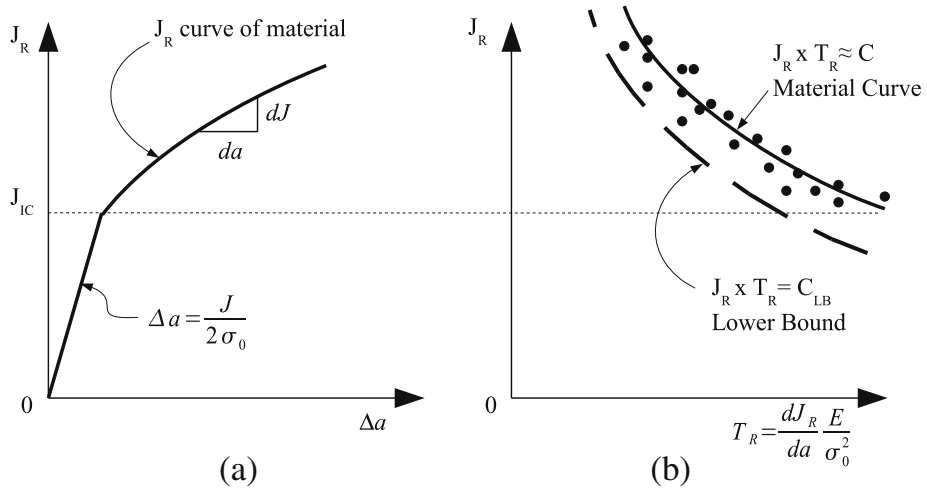

Fig. 1. Schematic illustration of (a) a *J*–*R* curve and (b) a *J*–*T* stability diagram.

2. The *J*-integral tearing stability method

The *J*-integral is defined in the usual manner with alternate forms [1] by:

$$J = \int_{\Gamma} \left(W dy - T_i \frac{\partial u_i}{\partial x} ds \right) = - \int_0^{\delta} \frac{\partial P}{\partial A} d\delta = \int_0^{P} \frac{\partial \delta}{\partial A} dP \tag{1}$$

where $W = \int_0^{\varepsilon_{ij}} \sigma_{ij} d\varepsilon_{ij}$, and T_i and u_i are corresponding components of traction and displacement on the contour, Γ, around the crack tip, dA is the crack area increment, δ is the load point displacement, P is the load and $dA = tda$, where t is the thickness and a the crack length. When the cracked section has reached its limit load for additional plastic deformation the J value at its tip can be approximated very well by:

$$J = - \int_0^{\delta} \frac{\partial P}{\partial A} d\delta = - \int_0^{\theta} \frac{\partial M}{\partial A} d\theta \cong - \frac{dM_L}{dA} \theta = J_{\text{applied}} \text{ (per unit thickness, } t) \tag{2}$$

where the limit moment in bending is M_L and θ is the angle of bending of the cracked section. This formula may be used to compute the increment or applied value of J_{applied} for a crack.

The materials resistance to the applied J shall be denoted as J_R (R for resistance) and is normally shown on a J_R vs. Δa diagram (where Δa is the change in crack length) which is called a material's resistance curve (Fig. 1a). It is an *Equilibrium* statement to say that:

$$J_{\text{applied}} = J_R \tag{3}$$

A crack becomes *Unstable* only if: $\frac{dJ_{appl}}{dA} \geqslant \frac{dJ_R}{dA}$, where $dA = tda$. This *Unstable condition* is better written as Eq. (4) where E is the elastic modulus and σ_0 is the flow stress.

$$T_{appl} = \frac{dJ_{appl}}{da} \frac{E}{\sigma_0^2} \geqslant \frac{dJ_R}{da} \frac{E}{\sigma_0^2} = T_R \tag{4}$$

T is denoted as the applied, T_{appl}, and resisting, T_R, tearing modulus. Eq. (4) is a more natural non-dimensional form for *Instability* determination [2–8]. Further, when judging instability it is often convenient to make use of a J vs. T diagram. The material's curve on such a *J*–*T* diagram can easily be bounded by a rectangular hyperbola for valid data (by ASTM specifications), that is: $J_R \times T_R = C$ (a material constant for a given thickness and temperature). Stability is ensured when the J_{appl}, T_{appl} point for a given loading or deformation is below and to the left of the material's curve. Fig. 1b shows a schematic of a J_R–T_R curve and the lower bounding material curve on a *J*–*T* diagram. These observations can be conveniently used to make stability judgments for cracks with remaining ligaments loaded well into the plastic range.

3. Stability of a crack in a fixed ended beam

Fig. 2 shows a fixed ended beam with a crack at its center section which has become fully plastic in bending.

The peak load is presumed to be applied and the question to be asked is will the crack be stable? If the crack then grows by an increment, da, one should ask whether the reduction in the moment, dM_L, causes an incremental increase in the bend angle, $d\theta$, at the cracked section, which in turn can cause divergent increments of additional crack growth. If only the cracked section is plastic, then the additional rotation at the cracked section is provided by further elastic rotation at the cracked

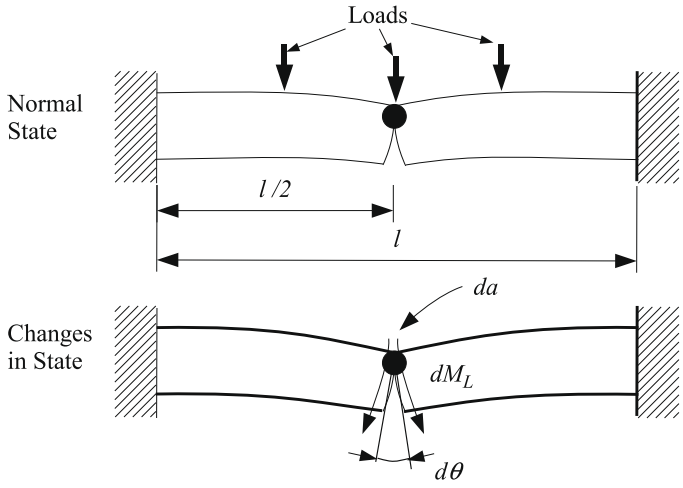

Fig. 2. A fixed ended beam loaded with a plastic hinge at the crack in its center section (can da cause dM_L, which causes $d\theta$ and further divergent increments of da).

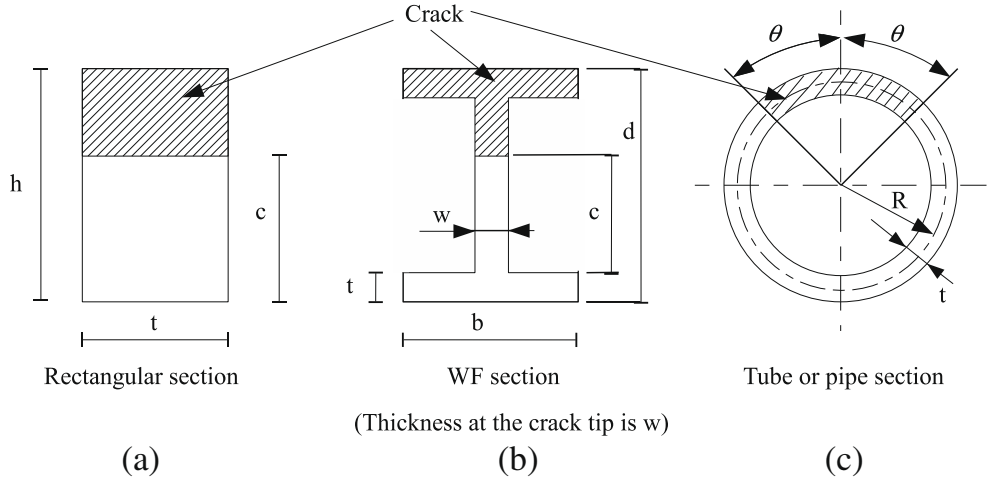

Fig. 3. Some typical cracked cross-sections subjected to fully plastic bending.

section caused only by the change in the limit moment, dM_L. For judging this, simple elastic beam theory gives Eq. (5), where E is the Young modulus, I the moment of inertia and l the length of the beam:

$$d\theta = \frac{dM_L l}{EI} \tag{5}$$

In order to consider stability, limit moment must be described. Fig. 3 shows some typical cracked cross-section as examples. Each one will be analyzed separately to note the pattern of results.

3.1. The rectangular cross-section

For a rectangular cross-section (Fig. 3a) the plane strain solution for the limit moment is the familiar Green and Hundy formula:

$$M_L = 0.35\sigma_0 c^2 t, \quad \text{where } I = \frac{h^3 t}{12} \tag{6}$$

and σ_0 is the flow stress, h is the section height, t is its width, and c is the remaining uncracked ligament. For this case the applied tearing modulus, T_{appl}, at limit moment is:

$$T_{appl} = \frac{E}{\sigma_0^2}\frac{dJ}{da}\bigg|_{appl} = \frac{E}{\sigma_0^2}\left[\frac{dJ}{d\theta}\frac{d\theta}{dM}\frac{dM}{da}\right]_{appl} = \frac{E}{\sigma_0^2}\left[\frac{dM_L}{dA}\frac{d\theta}{dM_L}\frac{dM_L}{da}\right] \tag{7}$$

The determination of the $\frac{dJ}{d\theta}$ in the first bracket is from Eq. (2). It is now noted that here $dA = tda = -tdc$ so that then:

$$\left(\frac{dM_L}{da}\right)^2 = 0.49\sigma_0^2 c^2 t^2 \quad \text{and} \quad \frac{d\theta}{dM_L} = \frac{12L_{effective}}{Eh^3 t} \tag{8}$$

where $L_{effective}$ will later be taken as the effective length of a beam equivalent to a fixed ended beam cracked at the center. Combining these results leads to Eq. (9) (for a rectangular beam of height, h). Order (1) means that for standard rectangular cross-section dimensions T_{appl} is approximately equal to L_{eff}/h.

$$T_{appl} \cong 6\left(\frac{c}{h}\right)^2 \frac{L_{eff}}{h} \cong \text{Order } (1)\frac{L_{eff}}{h} \tag{9}$$

3.2. For a wide flange section with a flange fully cracked

With a wide flange, Fig. 3b, in bending about its strong axis, the flange width is denoted, b, its thickness, t, the web thickness is w, and the total depth is d. If the tension flange is completely cracked and the crack extends into the web leaving a depth, c, of the web uncracked, the analysis proceeds as in the previous section. The limit moment is:

$$M_L = \sigma_0 cw\left(\frac{c+t}{2}\right), \text{ where } da = -dc \text{ or } dA = -wdc \text{ here, and } I \cong \frac{btd^2}{2} \tag{10}$$

The web is neglected in the moment of inertia, I, and in M_L the flange thickness, t, is neglected compared to c, which will be somewhat compensating errors. Combining these results following the steps of the previous section leads to Eq. (11) (for a WF section of depth, d). Again, Order (1) means that for standard WF cross-section dimensions T_{appl} is approximately equal to L_{eff}/d.

$$T_{appl} = 2\left(\frac{w}{t}\right)\left(\frac{c}{b}\right)\left(\frac{c}{d}\right)\frac{L_{eff}}{d} \cong \text{Order } (1)\frac{L_{eff}}{d} \tag{11}$$

3.3. The tube or pipe section with a through wall crack

A tube section is taken with a through wall crack extending over a sector of the section of 2θ in size (Fig. 3c). If the section is of mean radius, R, and thickness, t (with $t \ll R$) and becomes fully plastic then (where $dA = 2tda$):

$$\frac{dM_L}{da} = 2\sigma_0 th, \quad \text{where } h = R\left(\cos\theta + \sin\frac{\theta}{2}\right) \text{ and } I = \pi R^3 t \tag{12}$$

Again, proceeding as before (for a tubular section of diameter, D) Eq. (13) is obtained:

$$T_{appl} = \frac{4}{\pi}\left(\cos\theta + \sin\frac{\theta}{2}\right)^2 \frac{L_{eff}}{D} \leqslant 1.6\frac{L_{eff}}{D} = \text{Order } (1)\frac{L_{eff}}{D} \tag{13}$$

A more extensive analyses of cracked piping sections and their effective lengths is given in [9].

The trend noted here is clear that the T_{appl} for quite different cross-sections depends mainly on the beams effective length divided by its height. It is granted that more detailed analyses for each section could be computed. Moreover, from this simple analysis it has also been demonstrated as the crack gets deeper into each section, that the T_{appl} tends to diminish and if a crack does go unstable it is likely to be self-arresting. These trends are emphasized here to encourage further detailed analyses such as [9] which shows nuclear reactor piping cracks are normally always stable even with loads into the plastic range.

3.4. Fixed ended beam with crack not in the center of the beam

The preceding discussion assumed the crack location was at the center of a fixed ended beam. It shall now be appropriate to consider the non-symmetric case (Fig. 4) where the fully plastic cracked section is l_1 from one end and l_2 from the other end (or $l = l_1 + l_2$). Using simple elastic beam theory with a hinge at the crack location, the equivalent or effective length can be determined. The result is:

$$EI\frac{d\theta}{dM_L} = L_{eff} = l + \frac{3}{4}\left[\frac{\left(l_2^2 - l_1^2\right)^2}{l_1^3 + l_2^3}\right] \tag{14}$$

However, there is no such thing as a fixed ended beam. Normally a beam is framed into a structure that has elastic stiffness. Let the ends of the beam be framed into joints with rotational compliance equivalent to Eq. (15) where α_1 and α_2 are the non-dimensional compliance coefficients.

$$d\theta_1 = \left(\frac{\alpha_1 l_1}{EI}\right)dM_1 \quad \text{and} \quad d\theta_2 = \left(\frac{\alpha_2 l_2}{EI}\right)dM_2 \tag{15}$$

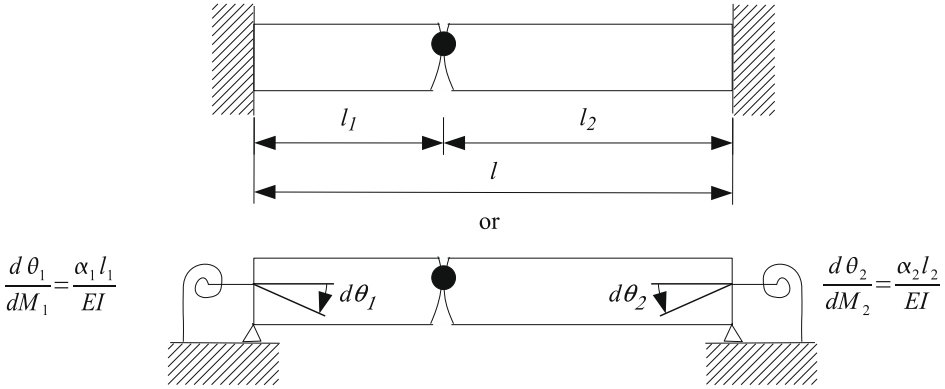

Fig. 4. Fixed ended or elastically rotationally supported beam ends.

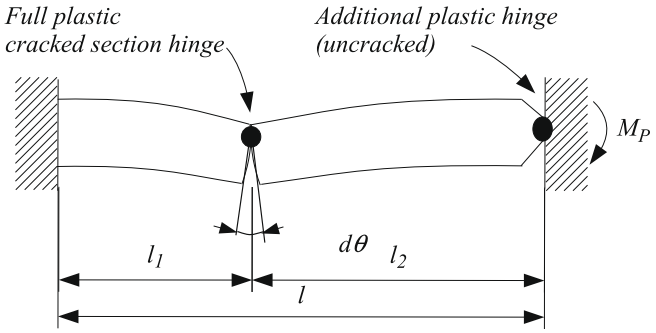

Fig. 5. A beam with a second plastic hinge in addition to one at the crack.

Adding these rotational compliances to the ends of the beam modifies the preceding relationship Eq. (14) into the following form:

$$EI\frac{d\theta}{dM_L}=L_{eff}=[l_1(1+\alpha_1)+l_2(1+\alpha_2)]+\frac{3}{4}\frac{\left[l_2^2(1+2\alpha_2)-l_1^2(1+2\alpha_1)\right]^2}{\left[l_1^3(1+3\alpha_1)+l_2^3(1+3\alpha_2)\right]} \tag{16}$$

It is noted that this form reduces to Eq. (14) for $\alpha_1 = \alpha_2 = 0$. It can be used to accommodate various elastic frames supporting the beam.

Further, for $\alpha_1 = \alpha_2 = 0$, let us suppose that an additional plastic hinge forms at the l_2 end of the beam, while the cracked section also remains fully plastic (Fig. 5), but with two plastic hinges the collapse mechanism is still not formed. For this case (Fig. 5) elastic beam analysis with these hinges gives:

$$EI\frac{d\theta}{dM_L}=L_{eff}=l_1\quad 1+\frac{l_1}{l_2}+\frac{l_1^2}{3l_2^2}+\frac{l_2}{3l_1}\Bigg) \tag{17}$$

It is equally easy to add examples of continuous beams with the second or more plastic hinges short of plastic collapse which is left undone here in order to proceed to more advanced examples of statically indeterminate structures.

4. Some special frames and a ring as examples of *L*-effective

Fig. 6 shows some frames and a simple ring of interest for further analysis. The two legged frame with differing stiffnesses for the beam, E_BI_B, and the columns, E_CI_C, with elastic bending theory leads to Eq. (18) for a centered crack in the beam, with length l, and a column height, h.

$$EI\frac{d\theta}{dM_L}=L_{eff}=l+\frac{E_BI_B}{2E_CI_C}h \tag{18}$$

For the square frame with each side of length, l, (Fig. 6) the result is:

$$EI\frac{d\theta}{dM_L}=L_{eff}=2l \tag{19}$$

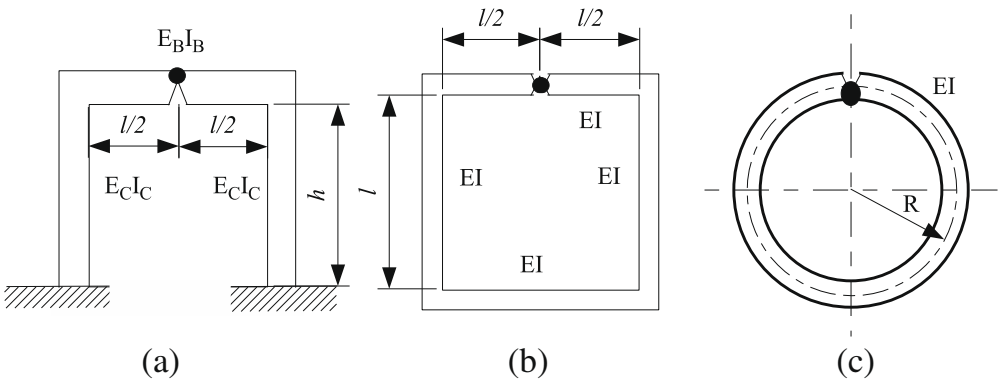

Fig. 6. Some frames and a ring for $\frac{d\theta}{dM_L}$ determination at the crack.

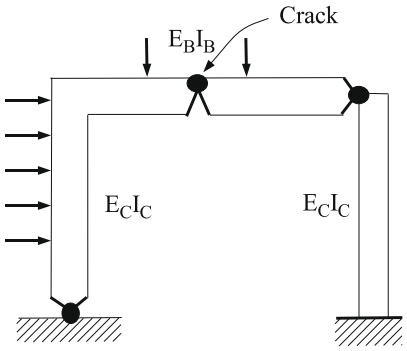

Fig. 7. A frame sustaining side-sway loading with two plastic hinges, as well as that at the crack.

which is not much of an increase of the effective length over a fixed ended beam. If this was part of a rectangular grid the two coefficient would be much closer to 1.

The problem of a ring of radius, R, has been discussed in [10] with the crack location at various angles from diametrically opposite concentrated loads. Therein the sequence of formation of plastic hinges was determined and the equivalent of the effective length was also determined for each case. Here, the treatment is with a plastic hinge at the crack location only to determine the effective length L_{eff}. Eq. (20) is obtained.

$$EI\frac{d\theta}{dM_L} = L_{eff} = \frac{2\pi}{3}R \tag{20}$$

Again, it is noted that the result is a little more than the diameter, $2R$, of the ring.

Finally, here let us come back to the first frame but, where typical side-sway induced additional plastic hinges are formed, as shown in Fig. 7. Again, this problem is analyzed using simple beam theory to obtain:

$$EI\frac{d\theta}{dM_L} = L_{eff} = \frac{4}{3}l + \frac{8}{3}\frac{E_BI_B}{E_CI_C}h \tag{21}$$

It is also noted here that the stiffnesses of columns in compression with large axial loads, P, should be adjusted by Eq. (22) where P_{cr} is the Euler critical load in compression.

$$E_CI_{C\text{-}effective} = E_CI_C\left(1 - \frac{P}{P_{cr}}\right) \tag{22}$$

5. Material properties needed to assure crack stability

The preceding discussion defined the material's tearing modulus as:

$$T_R = T_{\text{material}} = \left.\frac{dJ}{da}\right|_{\text{mat}}\frac{E}{\sigma_0^2} \tag{23}$$

where the values which may be used to evaluate crack stability can be determined from a material's J–R curve and elastic modulus and flow stress. It was also mentioned that empirically it has been noted that the J–R curve valid data will generate a part of a J vs. T diagram which can be conservatively enclosed by a rectangular hyperbola:

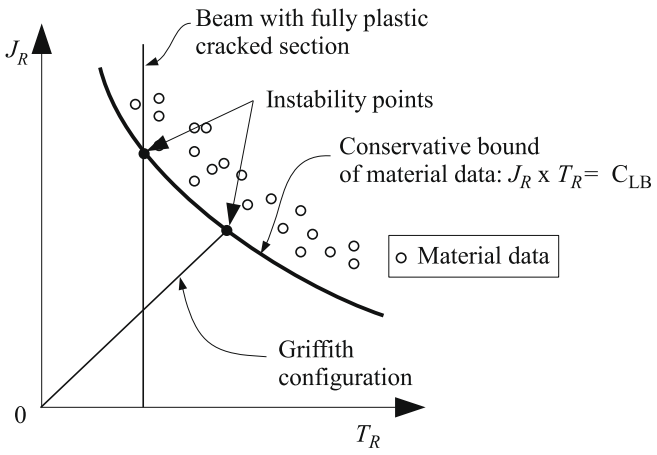

Fig. 8. A conservative bound of the material data, with the J_R vs. T_R shown for the Griffith configuration and beam analyses.

$$J_R \times T_R = J_{\text{mat}} \times T_{\text{mat}} = C \tag{24}$$

Normally, using these items to judge stability for well-designed structures, if cracked, will show very conservatively that crack stability can often be achieved. For example, consider an infinite sheet and with a central crack of $2a$ in length subjected to uniform tension, σ, perpendicular to the crack. This is the Griffith configuration, which, if large enough, can be treated by the usual elastic analysis. If a J–T diagram for the same thickness of material is bounded by the preceding rectangular hyperbola, the following Griffith equation can be employed:

$$J_{appl} = G = \frac{\pi\sigma^2 a}{E} \tag{25}$$

From this result it follows that:

$$T_{appl} = \frac{dJ_{appl}}{da}\frac{E}{\sigma_0^2} = \frac{\pi\sigma^2}{\sigma_0^2} \tag{26}$$

Combining these two previous equations leads to:

$$\frac{J_{appl}}{T_{appl}} = \frac{\sigma_0^2 a}{E} \tag{27}$$

which is a straight line of this slope through the origin of the J–T diagram as shown in Fig. 8.

For the various beam sections treated previously herein the results took the form:

$$T_{appl} = \text{Order } (1)\frac{L_{eff}}{D} \tag{28}$$

which are simply a vertical line on the J–T diagram as illustrated in Fig. 8. The intersections of these "applied curves" with the "material curve" indicates instability. For the Griffith configuration, it is noted that any increase the crack length results in a higher value of J at instability.

For an example in Ref. [9] it was noticed for typical nuclear piping systems that:

$$\frac{L_{eff}}{D} \cong T_{appl} = 11.2\text{—}62.7 \tag{29}$$

whereas the measured J-integral tests of this material gave:

$$T_{\text{mat}} = 205\text{—}452 \tag{30}$$

to very high values of J implying fully plastic action at cracked sections was easily reached with minor crack growth occurring. This practical example gives confidence that these analyses, although approximate, are very relevant.

In cases were doubt remains a final method, which does not even use the concepts of J-integral fracture mechanics, can be employed for practical engineering design. Experimentally, one can take a cracked section of the relevant beam and test it recording its moment vs. angle change curve for the cracked section. Then one has to compare the descending material $\frac{dM_L}{d\theta}$ like those found in the equations above from the structure's L_{eff}. If the material's $\left.\frac{dM_L}{d\theta}\right|_{\text{mat}}$ *is less than* the structure's $\left.\frac{dM_L}{d\theta}\right|_{\text{applied}}$:

$$\left.\frac{dM_L}{d\theta}\right|_{\text{mat}} < \left.\frac{dM_L}{d\theta}\right|_{appl} \tag{31}$$

then stability is assured. See Fig. 9 for an illustration of the test results.

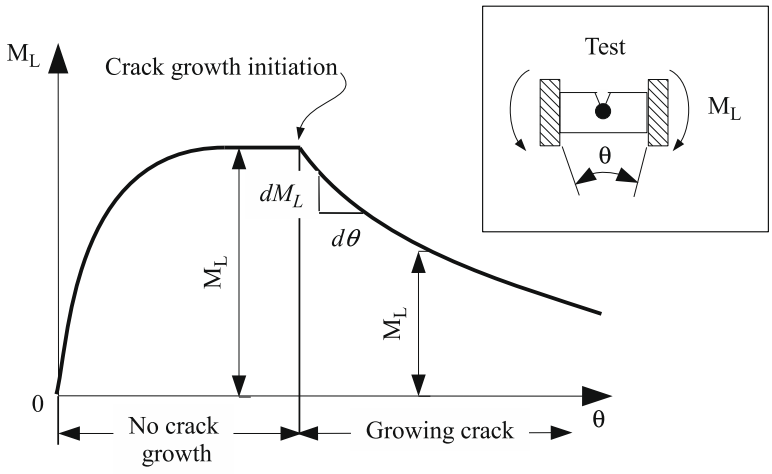

Fig. 9. An experimental approach with M_L vs. θ testing to avoid a J-integral approach.

6. Energy dissipation by plastic collapse mechanisms with cracks present

It is also of interest to compare the work dissipated by plastic hinges including those at cracked sections with those with cracks absent. Let us come back to the fixed ended beam studied in Section 3.4 (Fig. 5), but now, with a plastic hinge at each end, as illustrated in Fig. 10. This figure shows the collapse mechanism for such a fixed ended beam (or frame) where the collapse mechanism is entirely in one beam.

For the beam in Fig. 10 the work done with a crack at the central hinge is:

$$Work\ (cracked) = (M_P + M_L)(\theta_1 + \theta_2) = (M_P + M_L)\delta\left(\frac{l_1 + l_2}{l_1 l_2}\right) \tag{32}$$

where M_P is the fully plastic hinge moment of the uncracked section, and M_L is the hinge moment (i.e. the limit moment) of the cracked section. For the same mechanism without a crack at the central location, all the hinge moments are simply M_P. Therefore the ratio of the work cracked to uncracked is:

$$\frac{Work\ (cracked)}{Work\ (uncracked)} = \frac{M_P + M_L}{2M_P} = \frac{1}{2}\left(1 + \frac{M_L}{M_P}\right) \tag{33}$$

Now, if in Fig. 10 the crack location is instead at the l_1 end of the beam then the ratio of the work cracked to uncracked is:

$$\frac{Work\ (cracked)}{Work\ (uncracked)} = \frac{2l_1 + \left(1 + \frac{M_L}{M_P}\right)l_2}{2(l_1 + l_2)} \tag{34}$$

For both of these cases the minimum ratio is 1/2 to a maximum below 1.

Further, consider now the previous frame with a side-sway tendency present to develop a final hinge at the base of the other column as its collapse mechanism (Fig. 11).

For this mechanism with the cracked section in the central part of the beam the work is:

$$Work\ (cracked) = M_P\delta\left[\frac{\left(3 + \frac{M_L}{M_P}\right)l_2 + \left(1 + \frac{M_L}{M_P}\right)l_1}{l_1 l_2}\right] \tag{35}$$

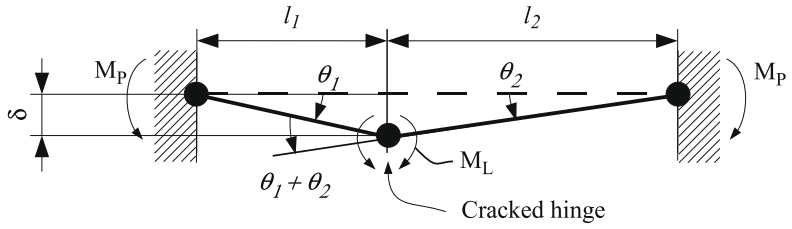

Fig. 10. A collapse mechanism for a fixed ended beam.

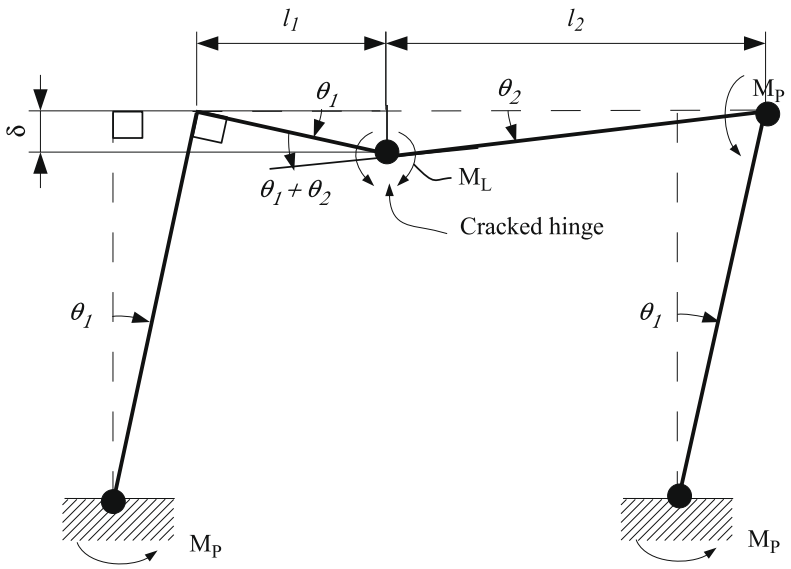

Fig. 11. A collapse mechanism for a frame with side-sway.

From this, setting $M_L = M_P$, the uncracked mechanism can be evaluated to get the work ratio of cracked to uncracked frame as in Fig. 11. It is:

$$\frac{Work\ (cracked)}{Work\ (uncracked)} = \frac{\left(1+\frac{M_L}{M_P}\right)l_1 + \left(3+\frac{M_L}{M_P}\right)l_2}{2l_1 + 4l_2} \tag{36}$$

The minimum ratio here must be more than 1/2 up closer to 1. Requiring a 4-hinged mechanism has caused that result. However, if not enough side-sway inducing loads are present the beam mechanism of Fig. 10 could be relevant instead for this frame.

In order to view these work ratios with a bit more perspective it is relevant to comment on the typical values of $\frac{M_L}{M_P}$ for the various cross-sections which has been already studied, and illustrated in Fig. 3, that are listed as follows:

(1) For the *rectangular section* cracked to 1/2 its depth the result is (for plane strain conditions):

$$\frac{M_L}{M_P} = 0.35 \tag{37}$$

(2) For the *wide flange* with the flange fully cracked:

$$\frac{M_L}{M_P} = \frac{1}{2}\left(\frac{w}{t}\right)\left(\frac{c}{b}\right)\left(\frac{c}{d}\right) = 0.28 \text{ (for typical proportions)} \tag{38}$$

(3) For a *tube or pipe section* with a through wall crack over a sector $2\theta = \frac{\pi}{2}$ or 90°:

$$\frac{M_L}{M_P} = 0.57 \tag{39}$$

Substituting these values into the previously stated work ratios gives further understanding of the absorption of energy for cracked structures where cracks can remain stable and collapse mechanisms are formed to enhance that absorption.

7. Conclusions

The application of *J*-integral tearing stability method to different typical cracked cross-sections of beams used in structural mechanical engineering has shown that T_{appl} is approximately equal to the ratio of an effective length, L_{eff}, over the characteristic dimension of the section (height for a rectangular section, diameter for a pipe for examples). Such *J*-integral analysis together with the simple elastic beam theory applied on some statically indeterminate frames and on a ring with plastic hinges allowed the assessment of the effective length L_{eff}. Finally, under bending the limit moment for a fully plastic

section with a crack, compared to the limit moment for uncracked section, is not negligible. The absorption of energy for cracked structures can be ensured by collapse mechanisms formed to enhance this absorption. Consequently, with tough material and good design to limit the effective length, as defined herein, it is possible to ensure stable crack growth even if plastic hinges appear. In such a case the fully plastic collapse mechanism must occur for complete catastrophic failure of the structure.

Acknowledgements

The authors acknowledge Arts et Metiers Paris Tech and Foundation Arts et Metiers for the financial support of the Prof. P.C. Paris' stay at LAMEFIP in 2008 and 2009. The encouragement of Prof. Ivan Iordanoff, Director of LAMEFIP, is also acknowledged with thanks.

References

[1] Rice JR. J Appl Mech 1968;35(June):379.
[2] Paris PC, Tada H, Zahoor A, Ernst H. The theory of instability of the tearing mode of elastic–plastic crack growth. In: Landes JD, Begley JA, Clarke GA, editors. Elastic plastic fracture. ASTM STP 668. ASTM; 1979. p. 5–36.
[3] Hutchinson JW, Paris PC. Stability analysis of *J*-controlled crack growth. In: Landes JD, Begley JA, Clarke GA, editors. Elastic plastic fracture. ASTM STP 668. ASTM; 1979. p. 37–64.
[4] Paris PC, Tada H, Ernst H, Zahoor A. Initial experimental investigation of tearing instability theory. In: Landes JD, Begley JA, Clarke GA, editors. Elastic plastic fracture. ASTM STP 668. ASTM; 1979. p. 251–65.
[5] Ernst H, Paris PC, Rossow M, Hutchinson JW. Analysis of load–displacement relationship to determine *J*–*R* curve and tearing instability material properties. In: Landes JD, Begley JA, Clarke GA, editors. Elastic plastic fracture. ASTM STP 668. ASTM; 1979. p. 581–99.
[6] Saxena A. Nonlinear fracture mechanics for engineers. CRC Press; 1998. p. 175–84.
[7] Joyce JA, Vassilaros MG. An experimental evaluation of tearing instability using the compact specimen. In: Fracture mechanics: thirteenth conference. ASTM STP 743; 1981. p. 525–42.
[8] Kaiser S, Carlsson AJ. Studies of different criteria for crack growth instability in ductile materials. ASTM STP 803; 1983.
[9] Paris PC, Tada H. The application of fracture proof design methods using tearing instability theory to nuclear piping systems postulating circumstances of through wall cracks, NUREG/CR-3464. Washington, DC: US Nuclear Regulatory Commission; September 1983.
[10] Young LJ, Paris PC, Tada H. The effects of a radial crack and its location on the development of plastic hinges and an analysis of crack stability in a circular ring with diametrically opposite concentrated loads. In: Ernst HA, Saxena A, McDowell DL, editors. Twenty second symposium. ASTM STP1131, vol. I. Philadelphia: ASTM; 1992. p. 793–808.